# Dalton Transactions

Accepted Manuscript






ROYAL SOCIETY OF CHEMISTRY

www.rsc.org/dalton

Cite this: DOI: 10.1039/c0xx00000x

www.rsc.org/xxxxxx

COMMUNICATION

# A dual-responsive "*turn-on*" bifunctional receptor: chemosensor for $Fe^{3+}$ and chemodosimeter for $Hg^{2+}$

**Sujay Mukhopadhyay[a], Rakesh Kumar Gupta[a], Arnab Biswas[a], Amit Kumar[a], Mrigendra Dubey[a], Maninder Singh Hundal[b] and Daya Shankar Pandey*[a]**

*Received (in XXX, XXX) Xth XXXXXXXXX 20XX, Accepted Xth XXXXXXXXX 20XX*
**DOI: 10.1039/b000000x**

**Synthesis of L1–L3, their thorough characterization by spectral as well as structural studies and use in selective photochemical detection of $Fe^{3+}$ and $Hg^{2+}$ at ppb level have been described. Notably, these exhibit bifunctional behaviour toward $Fe^{3+}$ (CHEF) and $Hg^{2+}$ (chemodosimetric) which has been unequivocally established by various studies.**

Development of highly selective and sensitive chemoreceptors for the detection of various cations have attracted sustained attention of several research groups because of its wide applications in diverse areas and imperative impact on the environment.[1] Iron is an essential element for human being and plays a vital role in diverse biological processes like oxygen carrier, uptake, metabolism, electron transfer and cofactor in many enzymatic reactions.[2,3] Iron deficiency in primary stages can cause anaemia, which may cause death by depriving organs of oxygen and an excess of iron also induces various diseases, such as Parkinson's, Alzheimer's disease and even cancer.[4] At the same time, mercury is one of the most prevalent toxic pollutants in the environment which has drawn a great deal of public attention. It is widely distributed in water and soil and its bio-accumulation in the living tissues of human and animal bodies *via* food chain causes serious health problems.[5] Both elemental and salt form of the mercury are converted to highly potent neurotoxin, methyl mercury *via* marine aquatic organisms.[6] Further, mercury ions cause a variety of diseases and affect the central nervous system even at very low concentration.[7] Extensive efforts have been made over past few decades to develop fluorescent chemoreceptors for various metal ions. However, these for $Fe^{3+}$ and $Hg^{2+}$, despite their indispensable role in many biochemical processes are still scarce.[7,8]

In addition, only a few highly selective and sensitive '*turn-on*' probes for the $Fe^{3+}$ and $Hg^{2+}$ have been reported due to their paramagnetic nature and coupling.[7,9] In general '*turn-on*' fluorescent probes are more efficient and advantageous over "*turn-off*" probes owing to the ease of detection at very low-concentration contrast relative to "dark" background.[10] In addition, colorimetric chemosensors also have attracted a great deal of attention for allowing 'naked-eye' detection in an uncomplicated and inexpensive manner, offering qualitative and quantitative information.[11] Fluorescence '*turn-on*' receptors are most often obtained by two main routes, chelation enhanced fluorescence enhancement (CHEF) where fluorescence enhancement occurs due to chelation of the ligand to metal centre and chemodosimeter wherein probe dissociates in presence of the host to generate a new fluorogenic species.[7] Further, CHEF is quite rare with $Hg^{2+}$ due to its inherent quenching nature, and in such cases chemodosimetric routes offer an excellent alternative.[7b,e]

With these points in mind through this work we have designed and synthesized three highly selective and sensitive dual-channel probes **L1**–**L3** for $Fe^{3+}$ and $Hg^{2+}$ by conjugating 2-aminophenylbenimidazole (**APBI**) and 2-chloro-7-methoxy-quinoline-3-carbaldehyde (**CMQC**) and its derivatives (Scheme 1). It has been clearly shown that these adopt two completely different routes toward recognition of the $Fe^{3+}$ and $Hg^{2+}$. To best of our knowledge, it presents the first report dealing with multi-analyte sensor for the detection of multiple ions with different spectral responses and mechanistic pathways, which may be a promising route to circumvent inconveniences associated with loading of multiple indicators.

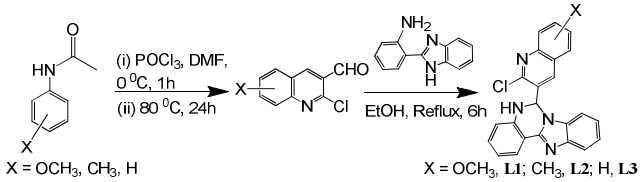


**Scheme 1**. Synthesis of **L1**, **L2** and **L3**.

The probes under investigation (**L1–L3**) have been thoroughly characterised by satisfactory elemental analyses, spectral (IR, $^1$H, $^{13}$C NMR, ESI-MS, UV–vis) studies. Relevant characterization data and spectra are given in ESI†. (Fig. S1–S5, Table S4-S5, ESI†) Structures of **L1**–**L3** have been unambiguously authenticated by X-ray single crystal analyses (Fig. 1).

$^1$H NMR spectra of **L1** and **L2** displayed singlet at $\delta$ 2.49 and 2.37 ppm, respectively associated with methoxy and methyl protons. The aromatic protons for **L1**–**L3** resonated in the range of 6.81–8.04 ppm. $^{13}$C NMR spectral data of the compounds under study further supported their proposed formulations and formation. Structures of all the probes have been determined by X-ray single crystal analyses.

Details about the data collection, structural solution, refinement, and selected geometrical parameters are gathered in

Table S1–S3 (ESI†). Pertinent views of the probes along with atom numbering scheme is depicted in Fig. 1.

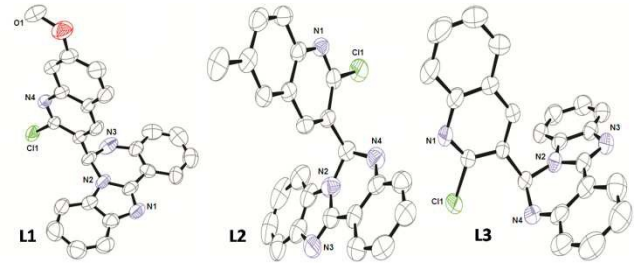


**Fig. 1** ORTEP views of **L1**, **L2** and **L3** with 50% ellipsoid probability. (Hydrogen atoms are omitted for clarity.)

Recognition behaviour of **L1**–**L3** toward various cations has been investigated by UV–vis absorption studies (Fig. S6a, S8 and S12 ESI†). In a typical experiment, solution of the cations *viz*. $Na^+$, $K^+$, $Ca^{2+}$, $Mg^{2+}$, $Al^{3+}$, $Mn^{2+}$, $Fe^{2+}$, $Fe^{3+}$, $Co^{2+}$, $Ni^{2+}$, $Cu^{2+}$, $Zn^{2+}$, $Cd^{2+}$, $Hg^{2+}$ and $Pb^{2+}$ (*c*, 100 mM, $H_2O$; nitrate salts) were added to a solution of **L1**–**L3** (*c*, 10 μM, $CH_3CN$ : $H_2O$, 1 : 1, v/v, HEPES buffer, pH = 7.2). Among these, only $Fe^{3+}$ and $Hg^{2+}$ exhibited significant changes in the absorption spectral behaviour of the probes. As depicted in Fig. 2a and 2b, gradual addition of $Fe^{3+}$ (0.0–6.0 equiv) to a solution of **L1** led to hyperchromic shift for absorption bands at ~ 290 – 345 nm and colour of the solution turned yellow from orange (Fig. 3). Unlike $Fe^{3+}$, very dissimilar spectral changes were observed for $Hg^{2+}$ (0.0–3.0 equiv). The band at 340 nm exhibited hypochromism and a new band emerged at ~400 nm. Isosbestic points at 302, 315 and 369 nm clearly indicated existence of more than two species in solution, with distinct colour change from orange to colourless (Fig. 3). The appearance of isosbestic points after addition of $Hg^{2+}$ may be due to reversible ring opening of the quinazoline scaffold, while its absence in presence of $Fe^{3+}$ due to weak interactions. It is noteworthy to mention that 6.0 equiv of $Fe^{3+}$ were required for saturation of **L1** while only 3.0 equiv of $Hg^{2+}$. The probes **L2** and **L3** exhibited similar spectral pattern under analogous conditions (Fig. S9, S13, Table S4, ESI†).

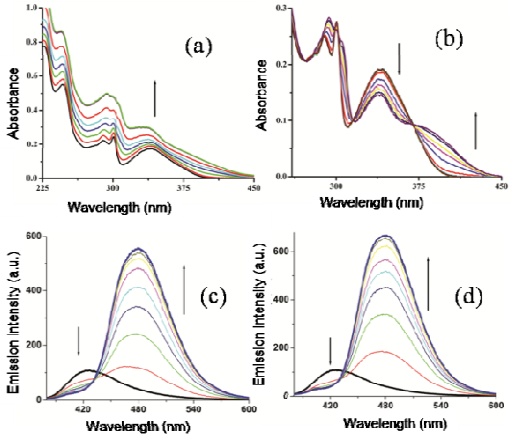


**Fig. 2** (a) UV–vis titration of **L1** with 6.0 equiv of $Fe^{3+}$, (b) UV–vis titration of **L1** with 3.0 equiv of $Hg^{2+}$, (c) Fluorescence titration of **L1** with 6.0 equiv of $Fe^{3+}$, (d) Fluorescence titration of **L1** with 3.0 equiv of $Hg^{2+}$.

The probes **L1**–**L3** (*c*, 10 μM, $CH_3CN$ : $H_2O$, 1 : 1, v/v, HEPES buffer, pH = 7.2) upon excitation at ~340 nm exhibit a weak emission band at ~425 nm ($\lambda_{ex}$ 340, 343, 349 and $\lambda_{em}$ 425, 410, 420 nm for **L1**, **L2, L3,** respectively). The fluorogenic response of these probes has been followed by monitoring the changes in fluorescence behaviour by addition of tested metal ions to a solution of **L1**–**L3**. Insignificant changes in the fluorescence behaviour of the probes were observed in presence of the tested metal ions except for $Fe^{3+}$ and $Hg^{2+}$ (Fig. S7a, ESI†). Gradual addition of $Fe^{3+}$ (0.0–6.0 equiv) to a solution of **L1** (Fig. 2c) resulted in a remarkable shift for the emission bands (425 to 478 nm) with ~3 fold increase in the quantum yield. It may be attributed to the coordination of quinazoline ring of the probe with the metal centre in a chelating mode. Similarly, addition of $Hg^{2+}$ (0.0–3.0 equiv) to a solution of **L1** (Fig. 2d) led to a large enhancement in the fluorescence intensity with a distinctive shift of 55 nm and an increase in the quantum yield by ~ 3.5 fold. To gain deep insight into binding mode of the **L1** with $Fe^{3+}$ and $Hg^{2+}$, UV–vis and fluorescence studies have been performed directly using **APBI**. Notably, it gave slightly different UV–vis and an analogous fluorescence spectrum with $Fe^{3+}$ (Fig. S16 ESI†). On the other hand $Hg^{2+}$ gave an analogous UV–vis and fluorescence spectral pattern. The emission pattern of **L1**–$\mathbf{Fe^{3+}}$ and **L1**–$\mathbf{Hg^{2+}}$ are similar due to the presence of the identical fluorophore **APBI**. It is worth mentioning that enhancement in the emission intensity in both the systems may be due to ring opening of the quinazoline scaffold followed by co-ordination with $Fe^{3+}$ and hydrolysis induced by $Hg^{2+}$. Due to the smaller ionic radius of $Fe^{3+}$ (0.785 A°) it may forms a stable complex **L1**–$\mathbf{Fe^{3+}}$ whereas $Hg^{2+}$ (0.830 A°) may not fit well into the cavity and results hydrolysis. Association constants ($K_a$) has been determined using Benesi–Hildebrand equation from the fluorescence titration curve for the receptor with $Fe^{3+}$ and are found to be 77 × $10^4$ $M^{-1/2}$, **L1**; 23 × $10^4$ $M^{-1/2}$, **L2**; 86.9 × $10^3$ $M^{-1/2}$, **L3** with good linear relationship (0.994, **L1**; 0.998, **L2;** and 0.994 **L3**) (Fig. S18, ESI†).[3] To verify our viewpoint, we have performed TDDFT calculations for **L1**, **APBI** and **CMQC** moieties and found that the absorbance behaviour of **L1** and **APBI** are almost identical and that of **CMQC** is slightly different, suggesting that identical emission pattern arises due to interaction of the metal ions ($Fe^{3+}$, $Hg^{2+}$) with **APBI** fluorophore. (Fig. S21, ESI†)

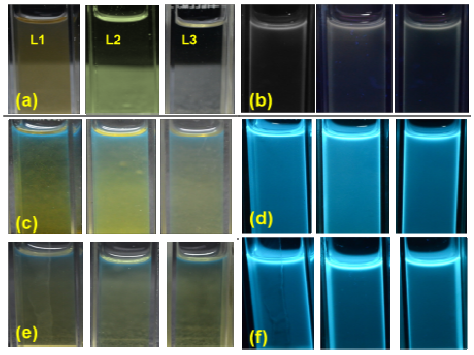


**Fig. 3** (a) Images showing probes under normal light, (b) probes under UV light 365 nm, (c) naked eye visible changes in presence of $Fe^{3+}$ (1 equiv), and (d) fluorogenic changes of same solutions, (e) naked eye visible changes in presence of $Hg^{2+}$ (1 equiv) and (f) fluorogenic changes of same solutions.

Job's plot analysis displayed 1 : 2 and 1 : 1 stoichiometries for

$Fe^{3+}$ and $Hg^{2+}$, respectively (Fig. S17, ESI†). The detection limits were calculated from the fluorescence experiment for both $Fe^{3+}$ (18.5, **L1**; 20.4, **L2**, 109.67 ppb **L3)** and $Hg^{2+}$ (1.98, **L1**; 2.27, **L2**, 13.33 ppb **L3**) (Fig. S19, ESI†). The excitation, emission wavelengths, changes in intensity and quantum yields for **L1–L3** are given in Table S4 (ESI†).

Selectivity and interference are two extremely important parameters while dealing with the evaluation of performance of a receptor. The selectivity and sensitivity of **L1** toward $Fe^{3+}$ and $Hg^{2+}$ have been determined by employing different metal ions ($Na^+$, $K^+$, $Ca^{2+}$, $Mg^{2+}$, $Al^{3+}$, $Mn^{2+}$, $Fe^{2+}$, $Co^{2+}$, $Ni^{2+}$, $Cu^{2+}$, $Zn^{2+}$, $Cd^{2+}$ and $Pb^{2+}$) in solution by both UV–vis and fluorescence method. The competition experiments have been conducted using 6.0 equiv of $Fe^{3+}$ in presence of other metal ions and the same concentration of **L1**. No noticeable changes were observed upon addition of other competing metal ions except $Hg^{2+}$. Addition of 3.0 equiv of $Hg^{2+}$ to a saturated solution of **L1**–$Fe^{3+}$ led alteration in the absorbance and emission behaviour of probes in the same way as $Hg^{2+}$ induced chromogenic and fluorogenic changes mentioned earlier. It indicated that the probe can be utilized conveniently for the detection of $Fe^{3+}$ by simple visual analysis, and is more selective toward $Hg^{2+}$ which in turn replaces $Fe^{3+}$. A comparative view of the absorbance and emission of **L1** upon addition of different co-existing metal ions (10.0 equiv) is shown in Fig. S6b, S6c, S7b, and S7c, ESI†. Fluorogenic behaviour of the probes **L2** and **L3** (Fig. S10, S11, S14, S15, ESI†) are almost similar to that of **L1**. Therefore, all these probes could be employed as a selective and sensitive colorimetric as well as fluorometric sensor for $Fe^{3+}$ and $Hg^{2+}$ ions.

One can have an idea about mechanistic aspects and efficiency of the systems from reversibility. To evaluate reusability of the receptors under investigation, reversibility behaviour of **L1** has been examined. In this context, both absorption and emission studies have been carried out using 6.0 equiv of $Fe^{3+}$, **L1** and an excess (50 equiv) of EDTA (ethylenediaminetetraacetic acid). Such an experiment revealed that colour of the solution turned yellow to orange with increasing concentration of EDTA with an attendant decrease in the emission intensity (Fig. S20a, S20c ESI†). It simply indicated the reversibility of the probe. On the other hand, significant changes were not observed after addition of EDTA to a solution of **L1** saturated with $Hg^{2+}$. It revealed that the probes behave as $Hg^{2+}$ induced chemodosimeters and changes are irreversible (Fig. S20b, S20d, ESI†). Based on these observations here we conclude that CHEF is responsible for fluorescence enhancement with $Fe^{3+}$ whereas, chemodosimetric hydrolysis for $Hg^{2+}$.

The receptors **L1**–**L3** are pH sensitive under acidic conditions. Therefore to examine the pH sensitivity, both UV–vis and emission studies have been carried out by aliquot addition of 1(N) HCl (pH ~ 7.2–4) and 1(N) NaOH (~ 7.2–10.5) to a solution of **L1**–**L3** (*c*, 10 μM) in $CH_3CN$ : $H_2O$ (1 : 1, v/v). The emission spectra showed insignificant changes in the emission intensity in pH range 4–10.5, indicating that system predominantly exist in its quinazoline form. Under strong acidic conditions (pH < 4) enhancement in the emission intensity, suggested protonation induced ring opening of the quinazoline along with a distinctive colour change from yellow to green.

Further, to verify interaction of **L1** with $Fe^{3+}$ and $Hg^{2+}$ metal nitrates $Hg(NO_3)_2{\cdot}H_2O$, $Fe(NO_3)_2{\cdot}9H_2O$ were reacted with **L1** in 1 : 1 $CH_3CN$ : $H_2O$ medium. The resulting products were washed with water and diethyl ether and analyzed by IR, $^1H$ NMR, and mass spectroscopic studies. A strong peak at 1384 $cm^{-1}$ suggested presence of $NO_3^-$ in **L1**–$Fe^{3+}$, while it is absent in **L1**–$Hg^{2+}$ (Fig. S22, S23, ESI†). Further, $^1H$ NMR titration studies have been carried out to acquire more information about the mode of interaction, complexation and hydrolysis between **L1**, $Fe^{3+}$ and $Hg^{2+}$. Addition of $Fe^{3+}$ (0.5–2.0 equiv) to a solution of **L1** resulted in recurrent broadening of proton signal (aromatic) for **L1** and suggested formation of a paramagnetic $Fe^{3+}$ complex **(L1**–$Fe^{3+}$**)** (Fig. S26, ESI†). Conversely, addition of 0.5–1.0 equiv $Hg^{2+}$ to a solution of **L1** led to occurrence of a new signal at $\delta$ 10.26 ppm, characteristic of aldehyde suggested rapid hydrolysis of **L1** (Fig. S27, ESI†).

ESI (–ve) mass spectrum of **L1**–$Fe^{3+}$ exhibited fragmented peaks at m/z 393.1389 (calcd. 396.4412) and 459.0800 (calcd. 460.0813) associated with **L1**–Cl+$H_2O$–3H, and **L1**–$CH_3$+$NO_3$–H, respectively. It also displayed a peak at 473.0961 (calcd. 474.0969) due to **L1**+$NO_3$–H. Above all it displayed a peak at 947.1888 (calcd. 947.1413) due to penta-coordinated Fe(III) complex + Li. Isotopic pattern for this peak corroborated well with calculated one (Fig. S24a, S25, ESI†). On the other hand, for **L1**–$Hg^{2+}$ peaks have been observed at m/z 208.9493 (calcd. 209.0953) and 288.9468 (calcd. 289.0937) corresponding to **APBI**–H and **APBI**+$NO_3$+$H_2O$–H. Further, peaks at m/z 429.0850 (calcd. 430.1197), 458.1028 (calcd. 459.0161) and 482.9693 (calcd. 484.9828) have been assigned to **L1**+$H_2O$, **CMQC**+Hg+2$H_2O$–H, and **CMQC**+Hg+$NO_3$–2H, respectively (Fig. S24b, ESI†). This study further suggested coordination of the quinazoline ring with $Fe^{3+}$ and hydrolysis in presence of $Hg^{2+}$.

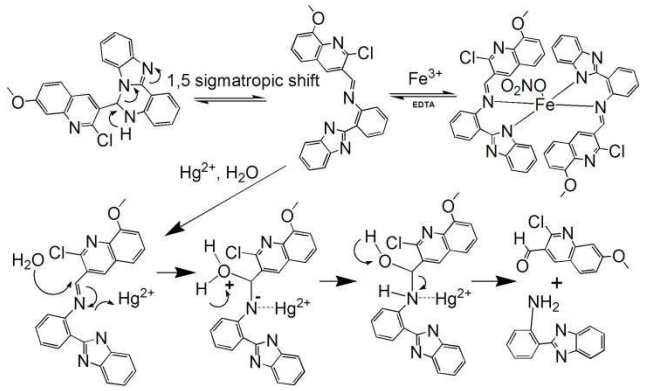


**Scheme 2**. Plausible mechanism for $Fe^{3+}$ complexation and $Hg^{2+}$ induced hydrolysis.

To further support the proposed structure of penta coordinated Fe(III) complex geometry optimization of **L1**–$Fe^{3+}$ have been performed using DFT calculations (Fig. 4a) by Gaussian 09. In the optimized structure of **L1**–$Fe^{3+}$ metal centre is coordinated with four nitrogen atoms from two units of **L1** (one each from the aldimine and deprotonated quinazoline) and exhibited square pyramidal geometry. The total energy of optimized structure converged to –102342.1 eV attesting the proposed structure as a stable product, not a transition state.

The ensuing product obtained from the reaction of $Hg^{2+}$ with

**L1**, was redissolved in acetonitrile, which upon slow evaporation afforded colourless crystals of **CMQC**. It has been characterized by X-ray single crystal analysis (Fig. 4b). Details about data collection, solution and refinement are summarized in Table S1 (ESI†) and a pertinent view of the compound is shown in Fig. 4b .The crystal data further authenticated chemodosimetric nature of the probe induced by $Hg^{2+}$.

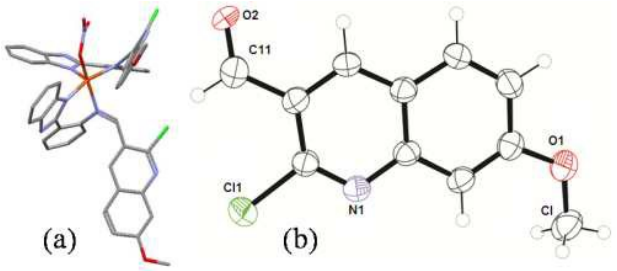


**Fig. 4** (a) Optimized structure of **L1**–$Fe^{3+}$ complex, (b) ORTEP view of **CMQC** with 50% ellipsoid probability.

From the above discussion we conclude that owing to smaller size of the $Fe^{3+}$ in comparison to $Hg^{2+}$, it can easily fit in the cavity of two quinazoline rings. Whereas large sized $Hg^{2+}$ experiences larger steric hindrance from the Cl–group of ligands, which in turn, hydrolyzes the probes to shed off the steric hindrance.

In conclusion, through this work we presented three new probes having the ability to detect $Fe^{3+}$ and $Hg^{2+}$ at ppb level in aqueous acetonitrile medium. These efficiently work in the pH range of 4–10.5, with insignificant interference of other metal ions. The probes behave as a chemosensor for $Fe^{3+}$ and chemodosimeter for $Hg^{2+}$ with greater sensitivity for $Hg^{2+}$. Although, small differences has been observed in emission intensity for these probes with $Fe^{3+}$ and $Hg^{2+}$, but these exhibit clear changes in UV–vis spectrum. Interestingly, dissimilar mechanistic approach of the probes toward $Fe^{3+}$ and $Hg^{2+}$ as chemosensor and chemodosimeter, respectively have been investigated for the first time in quinazoline system and can be further explored as a new pathway in metal ion sensing.

**Acknowledgment:** The authors gratefully acknowledges financial support from the Department of Science and Technology (DST), New Delhi, India for providing financial assistance through scheme [SR/S1/IC-25/2011] and also to UGC, New Delhi, India for the award of a Senior Research Fellowship 19-6/2011(i)EU-IV to S.M. We also thank Mr. S. Ghosh and Dr. B. Maiti, Department of Chemistry, Faculty of Science, BHU, Varanasi for extending help in DFT calculation.

## Notes and references

[a]*Department of Chemistry, Faculty of Science, Banaras Hindu University, Varanasi - 221 005 (U.P.) India. Fax: + 91 542 2368174; Tel: + 91 542 6702480; E-mail: dspbhu@bhu.ac.in*
[b]*Department of Chemistry, Guru Nanak Dev University, Amritsar-143005 (Punjab), India.*

† Electronic Supplementary Information (ESI) available: [Synthetic Methods and characterization data for all compounds, CCDC No. 1034021, 1034019, 1034022 and 1034020 and Photophysical data.]. See DOI: 10.1039/b000000x/

**1** (a) *Fluorescent Chemosensors for Ion and Molecule Recognition*; A. W.Czarnik, Ed.; American Chemical Society, Washington DC, 1993, p 1. (b) A. P. de Silva, H. Q. N. Gunaratne, T. Gunnlaugsson, A. J. M. Huxley, C. P. McCoy, J. T. Rademacher and T. E. Rice, *Chem. Rev.*, 1997, **97**, 1515−1566.

**2**. E. Beutler, V. Felitti, T. Gelbart and N. Ho, *Drug Metab. Dispos.*, 2001, **29**, 495–499. (b) D. Touati, *Arch. Biochem. Biophys*., 2000, **373**, 1–6. (c) G. Cairo and A. Pietrangelo, *Biochem. J.*, 2000, **352**, 241–250.

**3**. (a) S. Sen, S. Sarkar, B. Chattopadhyay, A. Moirangthem, A. Basu, K. Dhara and P. Chattopadhyay, *Analyst*, 2012, **137**, 3335–3342. (b) J. Huang, Y. Xu and X. Qian, *Dalton Trans*., 2014, **43**, 5983–5989.

**4**. (a) E. Beutler, V. Felitti, T. Gelbart and N. Ho, *Drug Metab. Dispos.*, 2001, **29**, 495–499. (b) G. Cairo and A. Pietrangelo, *Biochem. J*., 2000, **352**, 241–250.

**5.** (a) N. Zhang, G. Li, Z. Cheng and X. Zuo, *J. Hazard. Mater.*, 2012, **229–230**, 404–410. (b) J. Du, J. Fan, X. Peng, P. Sun, J. Wang, H. Li and S. Sun, *Org. Lett.*, 2010, **12**, 476–479. (c) S. Ou, Z. Lin, C. Duan, H. Zhang and Z. Bai, *Chem. Commun.*, 2006, 4392–4394. (d) B. N. Ahamed and P. Ghosh, Dalton Trans., 2011, 40, 12540–12547. (e) V. Bhalla, V. Vij, R. Tejpal, G. Singh and M. Kumar, *Dalton Trans*., 2013, **42**, 4456.

**6.** (a) M. Harada, *Crit. Rev. Toxicol*., 1995, **25**, 1–24. (b) H. N. Kim, W. X. Ren, J. S. Kim and J. Yoon, *Chem. Soc. Rev.*, 2012, **41**, 3210–3244.

**7.** (a) R. Pandey, R. K. Gupta, M. Shahid, B. Maiti, A. Misra and D. S. Pandey, *Inorg. Chem*., 2012, **51**, 298−311. (b) S. Mukhopadhyay, A. Biswas, R. Pandey, R. K. Gupta and D. S. Pandey. *Tet. Lett*., 2014, **55**, 1437–1440. (c) S. Kumar, P. Singh, G. Hundal, M. S. Hundal and S. Kumar, *Chem. Commun.,* 2013, **49**, 2667–2669. (d) X. Zhou, X. Wu, and J. Yoon, 2015, *Chem. Commun*., 2015, **51**, 111-113. (e) C. Bazzicalupi, C. Caltagirone, Z. Cao, Q. Chen, C. Di Natale, A. Garau, V. Lippolis, L. Lvova, H. Liu, I. Lundstrçm, M. C. Mostallino, M. Nieddu, R. Paolesse, L. Prodi, M. Sgarzi, and N. Zaccheroni. *Chem. Eur. J*. 2013, **19**, 14639 – 14653.

**8**. (a) K. Dhara, U. C. Saha, A. Dan, M. Manassero, S. Sarkar and P. Chattopadhyay, *Chem. Commun*., 2010, **46**, 1754–1756. (b) S. Mukherjee and P. Thilagar, *Chem. Commun.,* 2013, **49**, 7292–7294.

**9**. S. Ji, X. Meng, W. Ye, Y. Feng, H. Sheng, Y. Cai, J. Liu, X. Zhuc and Q. Guo, *Dalton Trans*., 2014, **43**, 1583−1588.

**10**. S. S. Nagarkar, T. Saha, A. V. Desai, P. Talukdar and S. K. Ghosh *Sci. Rep.*, 2014, **4**, 7053.

**11**. J.-R .Zhou, D.-P. Liu, Y. He, X.-J. Kong, Z.-M. Zhang, Y.-P. Ren, L.-S. Long, R.-B. Huang and L.-S. Zheng; *Dalton Trans*., 2014, **43**, 11579–11586.

# A dual-responsive "*turn-on*" bifunctional receptor: chemosensor for $Fe^{3+}$ and chemodosimeter for $Hg^{2+}$

Sujay Mukhopadhyay[a], Rakesh Kumar Gupta[a], Arnab Biswas[a], Amit Kumar[a], Mrigendra Dubey[a], Maninder Singh Hundal[b] and Daya Shankar Pandey*[a]

Synthesis of **L1**–**L3**, their thorough characterization by spectral as well as structural studies and use in selective photochemical detection of $Fe^{3+}$ and $Hg^{2+}$ at ppb level have been described. Notably these exhibit bifunctional behaviour toward $Fe^{3+}$ (CHEF) and $Hg^{2+}$ (chemodosimetric) which has been unequivocally established by various studies.